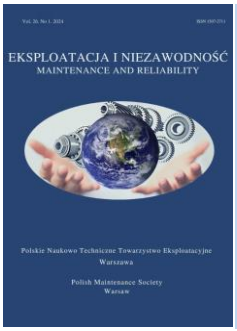

Eksploatacja i Niezawodnosc – Maintenance and Reliability
Volume 26 (2024), Issue 1
journal homepage: http://www.ein.org.pl

Article citation info:
Jaśkiewicz M, Evaluation of the Reliability of the Shoulder and Knee Joint of the KPSIT C50 Dummy Adapted to Crash tests carried out at low speeds., Eksploatacja i Niezawodnosc – Maintenance and Reliability 2024: 26(1) http://doi.org/10.17531/ein/178376

Evaluation of the Reliability of the Shoulder and Knee Joint of the KPSIT C50 Dummy Adapted to Crash tests carried out at low speeds.

Indexed by:
Web of Science Group

Marek Jaśkiewicz[a,*]

[a] [1]Faculty of Mechatronics and Mechanical Engineering, Kielce University of Technology, Poland

Highlights

- The durability and reliability of the joints of the KPSIT C50 dummy were assessed.
- The joints of the KPSIT dummy were compared with the joints of the Hybrid III 50th centil male dummy.
- The repeatability of the characteristics of the resistance moment in the joints depending on the cycles of measurements was demonstrated.
- The result shows the reliability and durability of the joints of the KPSIT C50 dummy.

Abstract

The article presents the results of experimental studies on the reliability and monitoring of the condition of the knee and shoulder joints of an anthropometric dummy designed for low-speed crash tests. Next, the characteristics of the resistance moments in the joints of the KPSIT C50 dummy are compared with the characteristics of the drag torque of the HYBRID III C50 dummy. The patented and manufactured knee and shoulder joints of the KPSIT C50 dummy characterized by a simple structure. The article presents a comparison of the resistance moments in the knee and shoulder joints of the KPSIT C50 dummy before crash tests and after a series of 200 crash tests. It has been shown that the patented solutions that have been used for low-speed crash tests do not need to be calibrated after a series of 5 crash tests, as is the case with the Hybrid III dummy. In addition, the results of experimental research presented in the article confirm the durability of the KPSIT C50 dummies joints and the possibility of using the joints for other centiles of anthropometric dummies.

Keywords
dummy reliability, exploitation of mannequin's joins, crash tests, anthropometric dummies.

1. Introduction

Anthropometric dummies, which reproduce individual parts of the human body, are used for crash tests. Tests performed with the use of dummies supply information what happens to each part of the human body when an accident occurs. Gerenal Motors' research on safety includes the search for new solutions and information on the safety of the driver, passengers, and especially children [1,2,3,4]. Anthropometric dummies are expected to be highly accurate and reliable when performing crash tests. The purpose of the dummies is to reproduce human behavior during a collision as best as possible. The biggest threat to the implementation of crash tests is the lack of repeatability of results and possible damage, especially to the joints of the dummy. The lack of reproducibility of results is related to the structure of anthropometric dummies [5,6,7]. While the lack of repeatability and inconsistency of motion characteristics can be eliminated through calibration, the strength of the joints is not. According to the manufacturer's data, the Hybrid III dummies must be checked before the crash test, while the joints must be calibrated to maintain repeatability of results and avoid possible measurement errors [8,9,10].

In the first years, human corpses and animals such as pigs were used for crash tests [11]. Volunteers also took part in the

(*) Corresponding author.
E-mail addresses: M. Jaśkiewicz (ORCID: 0000-0002-0032-9477) m.jaskiewicz@tu.kielce.pl,

crash tests. Unfortunately, experiments on pigs and human carcasses were not satisfactory, as the data supplied to scientists turned out to be not very reproducible. The solution was "anthropomorphic test devices (ATDs)", now better known as crash test dummies [12,13,14].

Before anthropometric dummies became the standard for crash testing, they had to go a long way in improving their design and data collection. The origins of anthropometric dummies used for crash tests date back to the 1920s, when vehicles began to gain more and more popularity, and the number of road accidents and casualties began to increase steadily [15,16,17]. The first dummywas patented in 1949 by Samuel W. Alderson [18]. At that time, crash tests were a novelty, there was a lack of reliable data on the impact of forces on the human body. At that time, there were no tools to measure such impacts [19,20,21].

The breakthrough came in 1977 with the launch of the Hybrid III. It has become a standard dummy in the automotive industry. The dummy Hybrid III is continuously improved by Humanetics and remains the primary crash test dummy. It differs from the previous generation model mainly in the more advanced design of the neck and individual parts of the human body. Additionally, Hybrid III is available in a wider range of sizes than previous crash test dummies. Hybrid III family dummy have high biofidelity with the human body [22,23,24].

Research on the behavior of dummies during crash tests, taking into account their similarity to the human body, has led to the development of procedures for assessing injuries to the head, face, chest, abdomen, lower and upper limbs, which are used by all manufacturers around the world [25,26]. The joints used in the crash test anthropometric dummy (Hybrid III) must be removed, calibrated, and reinstalled after several crash cycles.

For dummies representing men or women at the 50th percentile, the differences in joint structure are less visible, but

for dummies representing children, the joint structure is different [27,28,29]. The dummies, representing children aged 12 and 6, have simple joint structures. In the case of a dummy depicting a 3-month-old baby, the shoulder joints resemble the structure of a child's doll. However, the elbow or knee joint does not occur at all. The upper and lower limbs constitute one element.

It should be noted that the ideal design solution for dummy would be a solution that would ensure the lack of frequent calibration and the durability and reliability of the joints. [30,31,32].

The purpose of using dummies in crash experiments is to reduce the number of deaths caused by traffic accidents [33,34,35]. The topic of traffic accidents is discussed in articles [36,37,38,39]. It should be noted that thanks to dummies, it is possible to predict the likelihood of people being injured in a road accident [40,41,42,43].

The next part of the article presents the design assumptions of the KPSIT C50 shoulder and knee joints, the characteristics of the drag torque in the KPSIT C50 joints, which were compared with the Hybrid III dummies, and the torque resistance characteristics of the KPSIT C50 dummies after a cycles of crash tests.

2. Innovative joints KPSIT C50 Dummy

The main assumption for the construction of the KPSIT dummy was that all parts of the dummy should correspond to the shape and weight of the human body. Figure 1 shows the KPSIT C50 dummy, representing the 50th percentile male.

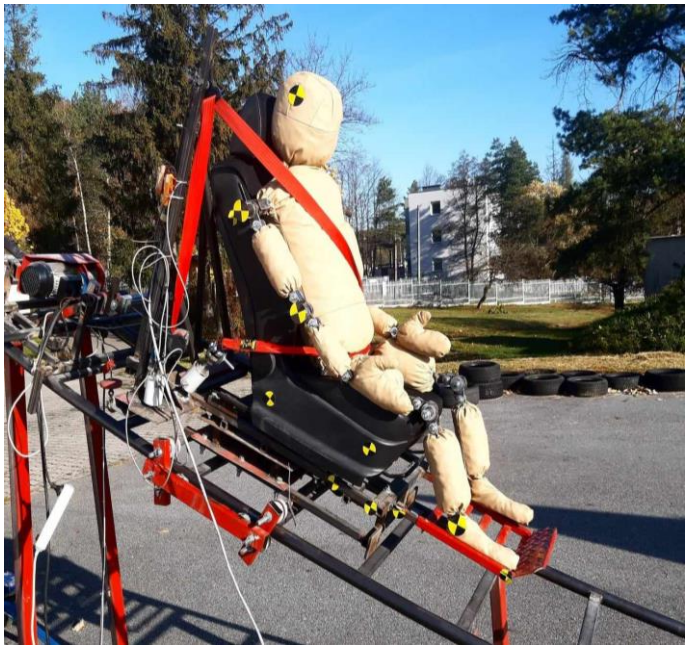

Fig. 1. KPSIT C50 dummy.

The main assumption of the construction of the KPSIT physical dummy is to reproduce the dynamics described by the characteristics of the moments of resistance of individual joints of the human body (Hybrid III 50th centil male dummy). One of the main assumptions of the dummy design was a simple

procedure of replacing a damaged joint with a new one. All physical dummy joints are quickly and easily removed so that they can be replaced with a new joint. All physical dummy joints have the ability to adjust the resistance, making them versatile and can be used for anthropometric dummies representing different percentiles of both male and female populations.

Each joint is equipped with a set of ball bearings and a joint housing that protects it from damage. The compression spring is responsible for the shape of the corresponding stiffness characteristics. The advantage of this design solution over physical dummy joints is that the joints are not permanently connected to any part of the dummy's body, making it easy to replace damaged components with new ones. In contrast to the male Dummy Hybrid III 50th Centil, its joints are permanently attached to parts of its body.

Repair of individual joints in the KPSIT dummy involves the replacement of the ball bearing or the entire bearing with its housing. To disassemble them, it is enough to unscrew the two screws attaching the joint to individual parts of the mannequin's body. Correct operation of the designed mannequin joint does not require disassembly and calibration after a specified number of test cycles. The only check that needs to be done is to check the alignment of the bolt that presses the spring against the joint.

Remember that the shoulder joint is a ball and socket joint that connects the upper limb to the human torso. The advantage of the shoulder joint design solution is that damaged elements can be easily replaced with new ones.

The ball bearing is part of the first part of the joint. It is the main element in it. The bearing is placed in a steel housing, which protects the bearing against damage. The joint allows simple assembly to the dummy structure using two screws. The second part of the joint consists of a steel pipe with a locking cam. A security hole is made in the back of the steel pipe. A steel bolt is placed in the security hole to protect the joint from slipping out and damaging the ball bearing. At the beginning of the steel pipe, holes were made for mounting the tension springs and the main hole for mounting the third element of the joint. The third element of the designed joint is the dummy arm. The upper part of the arm has holes for mounting tension springs and a main hole for connecting the arm to the steel pipe of the designed joint. The KPSIT C50 shoulder joint is shown in Figure 2.

Fig. 2. KPSIT C50 Dummy Shoulder Joint.

The shoulder joint allows flexion and extension movement consistent with the movement of the human body. A locking cam located in the shoulder edge prevents damage to the joint and prevents further movement beyond the range of motion of the human shoulder joint.

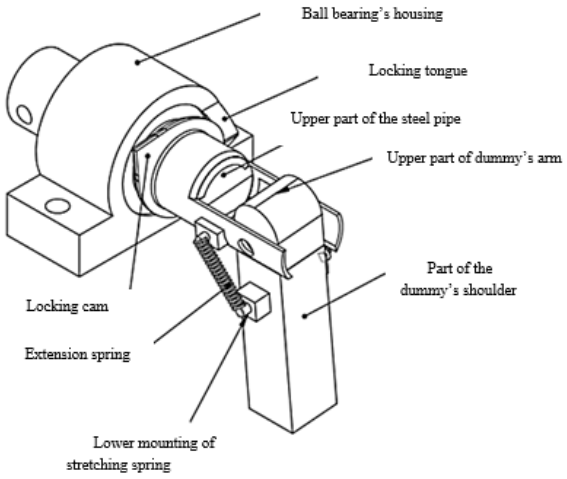

Fig. 3. Shoulder Joint KPSIT C50 Physical Dummy.

Abduction movement in the shoulder joint is possible thanks to the use of tension springs. Tension springs connect the second element of the shoulder joint to the third. The joint design prevents damage to the tension springs. The maximum range of motion of the shoulder joint during the abduction movement

ends when the upper part of the arm touches the steel tube of the second element of the shoulder joint. The second and third elements of the shoulder joint are connected with a steel screw. This connection is stabilized by tension springs. The appropriate selection of springs ensures stiffness similar to the human shoulder joint. The shoulder joint of the dummy has two degrees of freedom. Allows movement of the upper tips towards the X axis (longitudinal) and towards the Z axis (vertical). Figure 3 shows the shoulder joint of a KPSIT dummy, which consists of three elements connected together.

Figure 4 shows the left part of the designed elbow joint of the manikin. Figure 5 shows the right part of the designed elbow joint of the manikin. The elbow, knee and thigh joints of the physical manikin have one degree of freedom. The joints enable movement towards the X axis. Figure 6 shows the knee joint of the KPSIT C50 dummy.

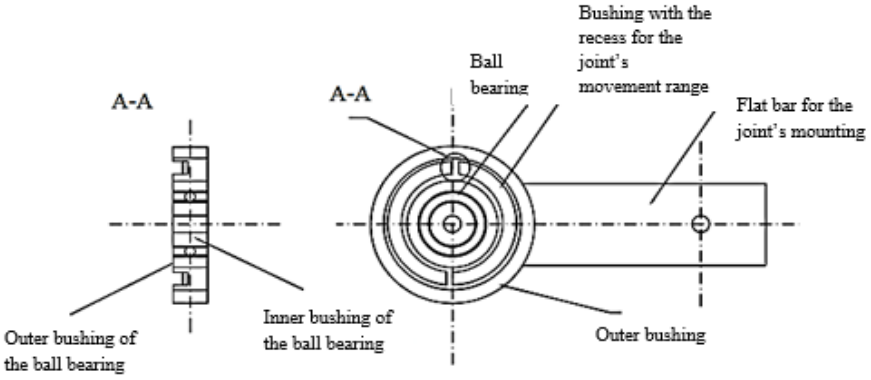

Fig. 4. The left part of the designed elbow joint.

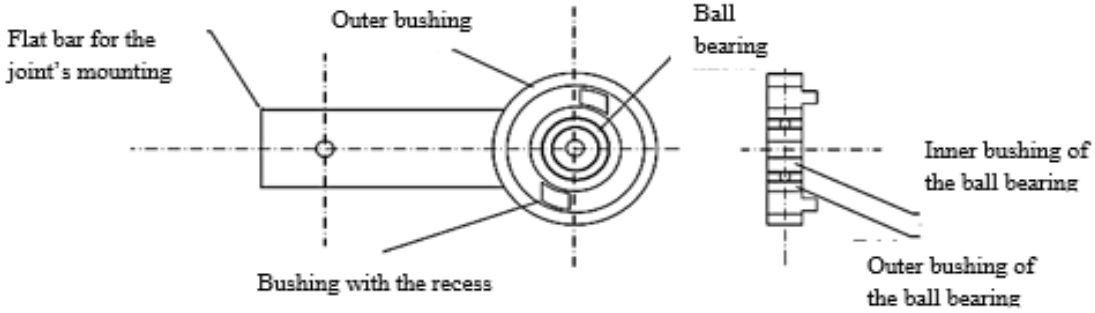

Fig. 5. The right part of the designed elbow joint.

Fig. 6. Knee Joint KPSIT C50 Dummy.

The designed joints have resistance torque characteristics that are comparable to those of a human joint. By appropriately tightening the mounting screw on which the spring is located, the moment of resistance in the joint is changed. This solution allows you to adjust the moment of resistance in the wrist to each percentile of the population. The spring on the mounting screw is separated by spring washers. The use of spring washers allows the joint to move freely without changing the position of the spring. Both the design of the shoulder and knee joints are covered by the patent protection of the Republic of Poland [30,31].

3. Data and research methods

A strain gauge force sensor was used to characterize the moment of resistance in the joints. The characteristics of the resistance

moment were made on the basis of point measurements occurring in particular ranges of motion. To measure the range of motion, a protractor was used, which was placed in the central point of the joint mounting screw. On the basis of the test results, the moment of resistance in the individual joints was determined. The moment of resistance is represented in the form of equation 1 [30, 31, 36]. An example of the course of the components of the moment of resistance is shown in Figure 7.

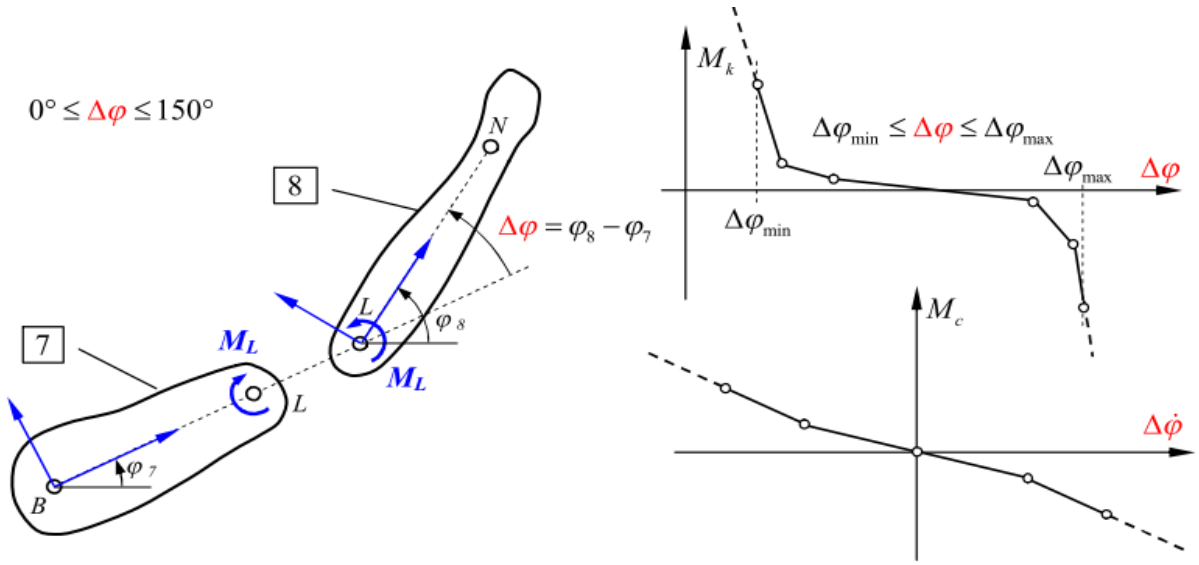

Fig. 7. An example of the course of the components of the moment of resistance [30].

$$M = M_k(\boldsymbol{\Delta\varphi}) + M_c(\boldsymbol{\Delta\dot{\varphi}}) + C \quad (1)$$

Where:

$M_k(\boldsymbol{\Delta\varphi})$ — a component that is a function of the joint angle,

$M_c(\boldsymbol{\Delta\dot{\varphi}})$ — component that is a function of the angular velocity at the joint,

$C = M_o - M_k(\boldsymbol{\Delta\varphi_o})$ — constant selected on the basis of initial conditions,

$M_0, \Delta\varphi_o$ — torques and initial joint angles.

Figure 8 shows an example of attaching a strain gauge to the elbow joint of a physical dummy KPSIT C50. Figure 9 shows the strain gauge used in the research.

Fig. 8. Strain gauge mounted on the example of the elbow joint of a 50th percentile male physical dummy.

Fig. 9. Strain gauge used in research.

The characteristics of the moment of resistance were compared with the characteristics of the moment of resistance of the Hybrid III 50th centil male dummy. The research and determination of the characteristics for the Hybrid III 50th percentile dummy were carried out at PIMOT and presented in the papers [31,32] The characteristics of the torque of resistance of the shoulder joint of the KPSIT C50 physical dummy coincide with the stiffness values of the Hybrid III 50th centil

male dummy in 85%. The negative values of the drag torque, which determine the backward movement of the joint, are 99 % the same as those of the Hybrid III. Differences between the resistance torque characteristics are evident in the case of positive values. The largest difference in the moment of resistance occurs at a tilt angle of 50° and amounts to 10 Nm. Figure 10 shows the characteristics of the moment of resistance of the shoulder joint of the KPSIT C50 dummy.

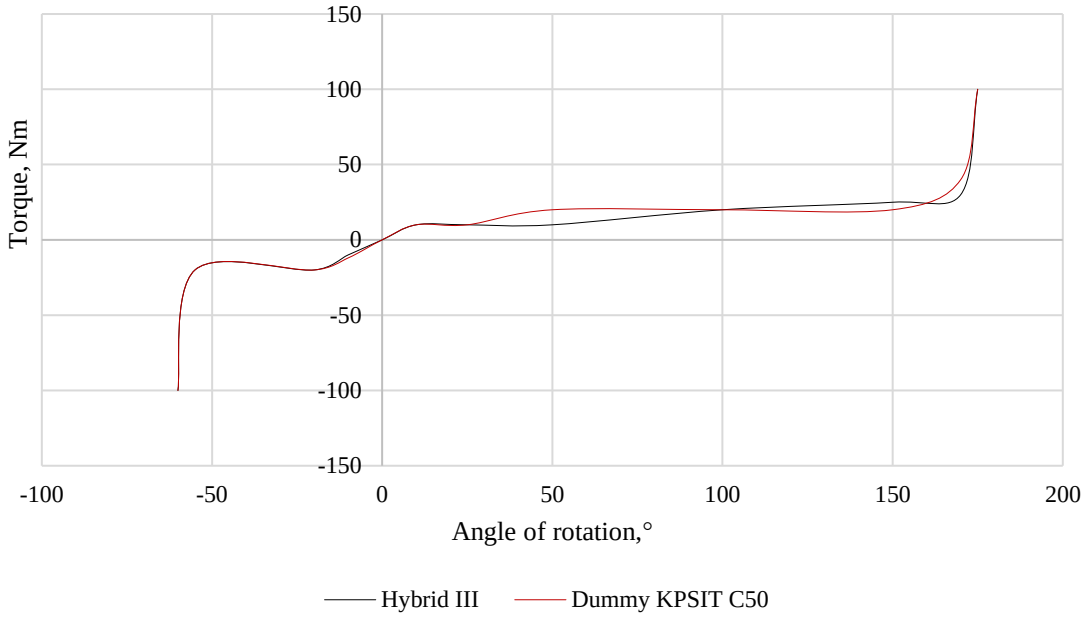

Fig. 10. Characteristics of the torque of resistance in the shoulder joint of the KPSIT C50 dummy.

The torque resistance characteristics of the KPSIT C50 knee joint coincide with the stiffness values of the Hybrid III 50th centil male dummy by 95 %. The differences occur in the final stage of the rotation angle, both with positive and negative values, and their values differ from each other by 5 Nm. The characteristics of the drag torque in the knee joint of the KPSIT C50 physical dummy are shown in Figure 11.

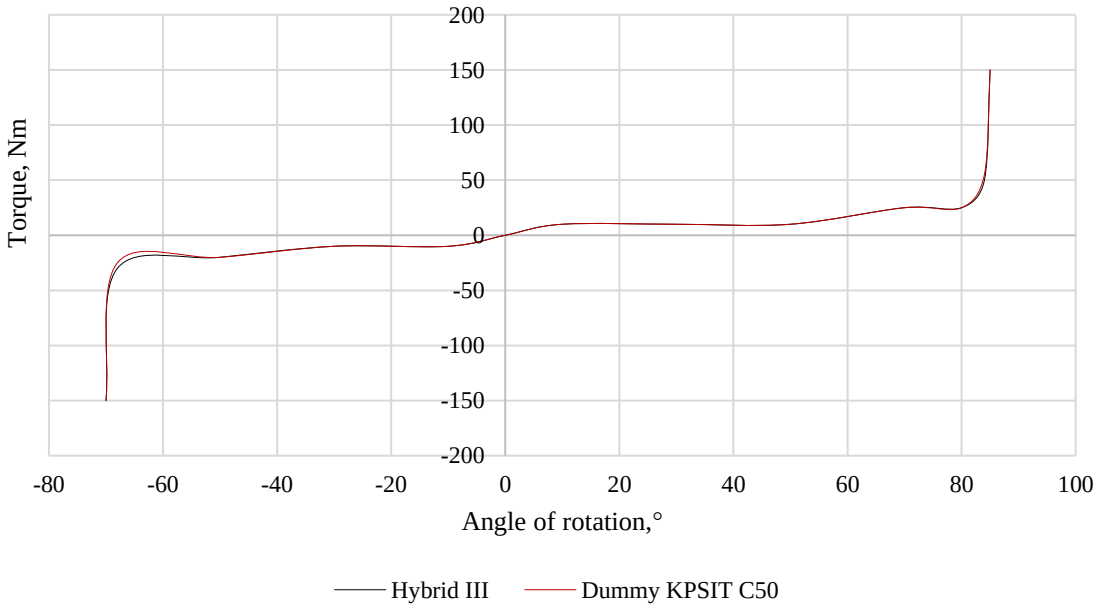

Fig. 11. Characteristics of the torque of resistance in the knee joint of the KPSIT C50 dummy.

4. Results and discussion

Satisfactory results of the similarity of the moments of resistance in the shoulder and knee joints of the KPSIT C50 physical dummy allowed for the implementation of a cycles of crash tests at low speed. The dummy was used for front, rear, and side tests at low speeds from 15 km/h to 20 km/h. Figure 12 shows the KPSIT C50 dummy taking part in a rear crash test using a sports seat. Figure 13 shows the KPSIT C50 dummy taking part in a frontal crash test using a passenger vehicle seat. Figure 14 shows the KPSIT C50 dummy taking part in a frontal crash test using a bus seat.

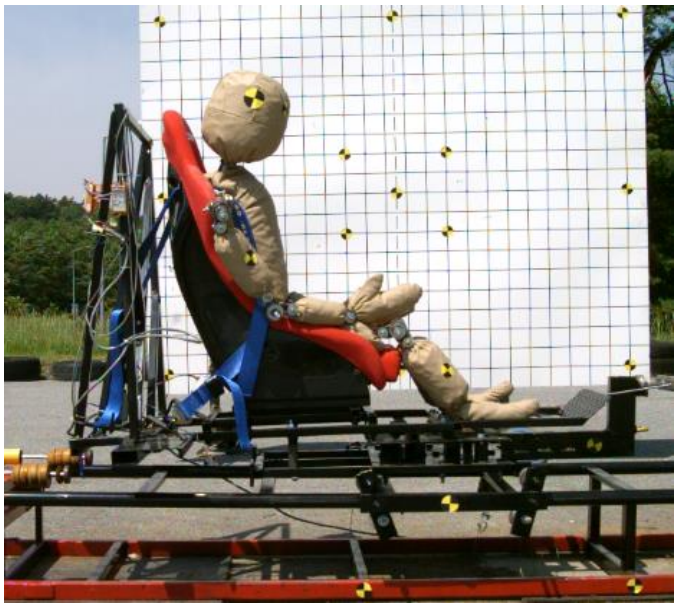

Fig. 12. KPSIT C50 dummy taking part in a frontal crash test using a passenger vehicle seat.

Fig. 13. KPSIT C50 dummy taking part in a frontal crash test using a passenger vehicle seat.

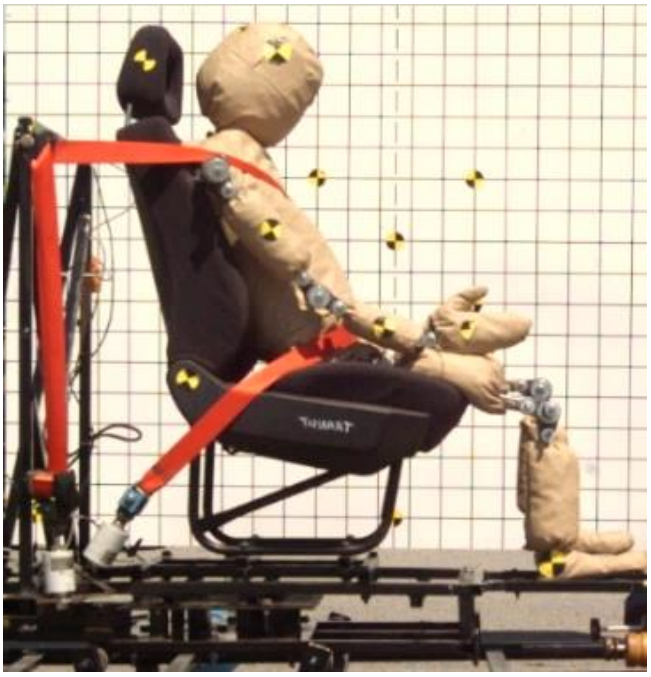

Fig. 14. KPSIT C50 dummy taking part in a frontal crash test using a bus seat.

Over the course of 24 months, the KPSIT C50 physical dummy has undergone a cycles of 200 crash tests. The drag torque characteristics of the patented joints were checked each time after a cycles of 25 crash tests. The characteristics of the drag torque in the shoulder joint of the KPSIT C50 dummy are shown in Figures 15 to 23. The characteristics of the drag torque in the shoulder joint of the KPSIT C50 dummy, taking into account all cycles of crash test measurements, are shown in Figure 24.

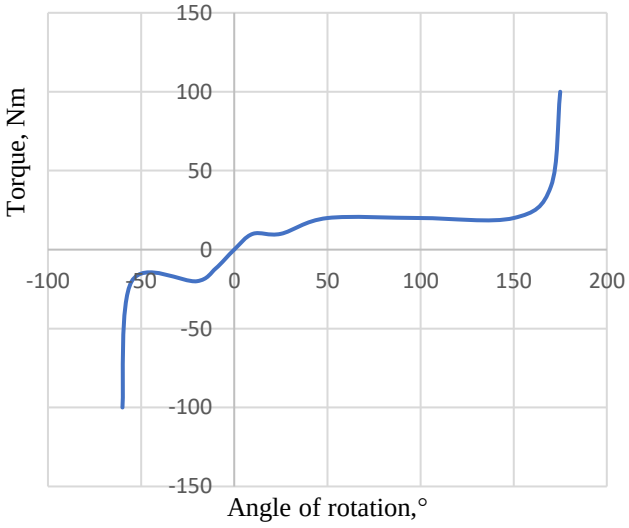

Fig. 15. Characteristics of the drag torque in the shoulder joint of the KPSIT C50 dummy – before the first crash test.

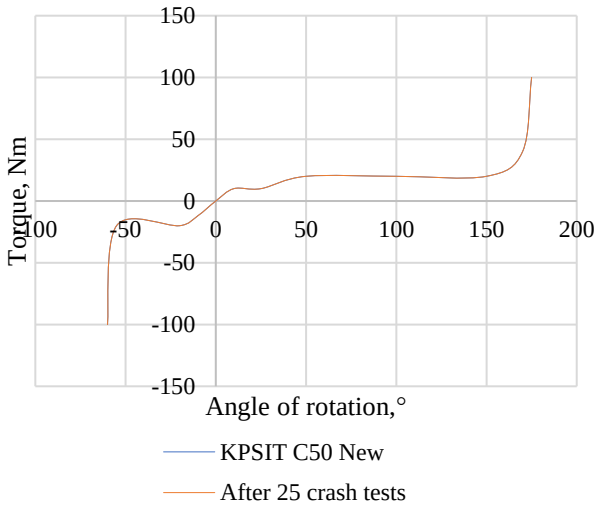

Fig. 16. KPSIT C50 Shoulder Joint Drag Characteristics – After 25 Crash Tests.

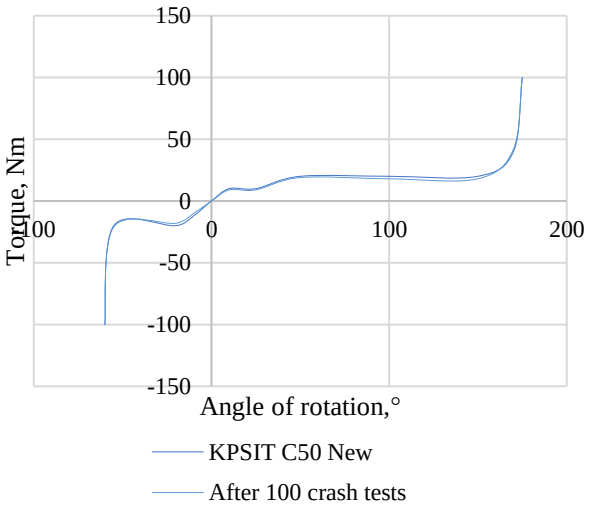

Fig. 19. Characteristics of the drag torque in the shoulder joint of the KPSIT C50 dummy – after 100 crash tests.

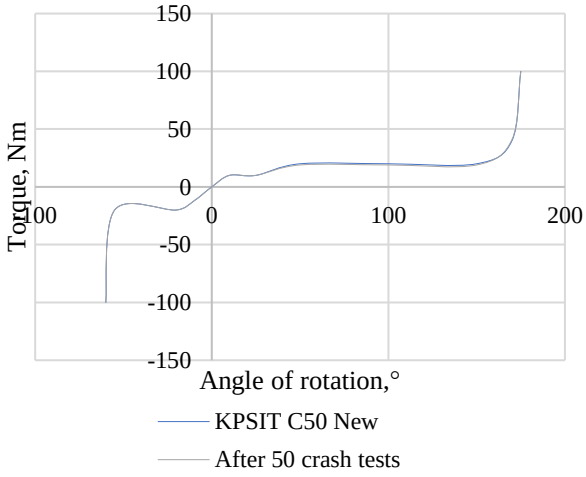

Fig. 17. Characteristics of the drag torque in the shoulder joint of the KPSIT C50 dummy – after 50 crash tests.

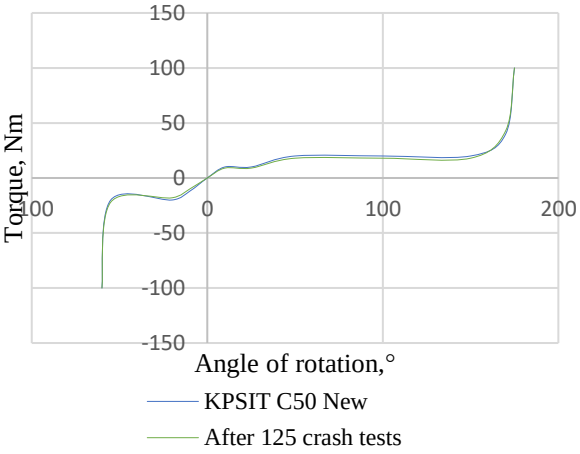

Fig. 20. Characteristics of the drag torque in the shoulder joint of the KPSIT C50 dummy – after 125 crash tests.

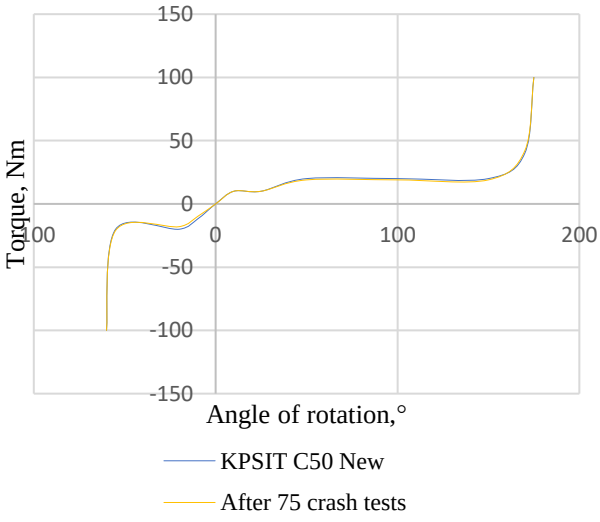

Fig. 18. Characteristics of the drag torque in the shoulder joint of the KPSIT C50 dummy – after 75 crash tests.

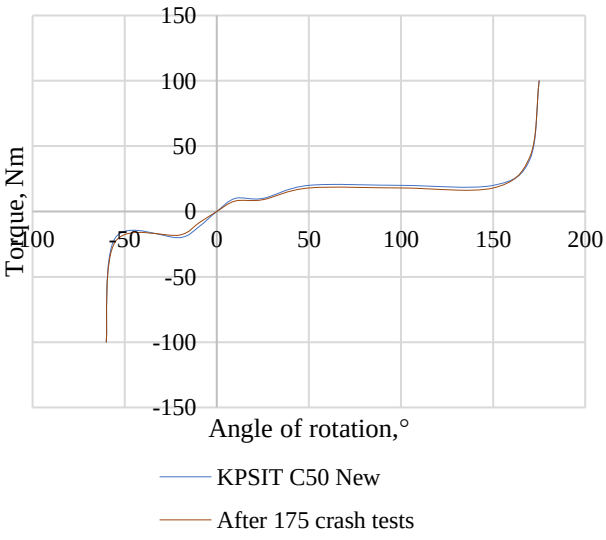

Fig. 22. Characteristics of the drag torque in the shoulder joint of the KPSIT C50 dummy – after 175 crash tests.

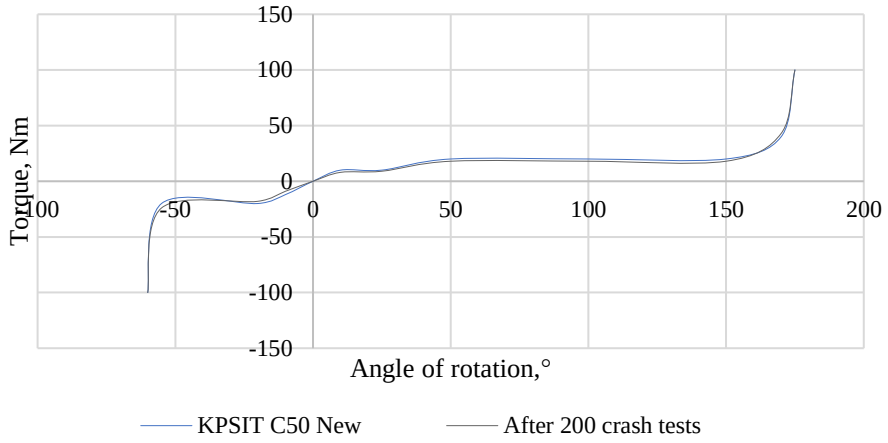

Fig. 23. Characteristics of the drag torque in the shoulder joint of the KPSIT C50 dummy – after 200 crash tests.

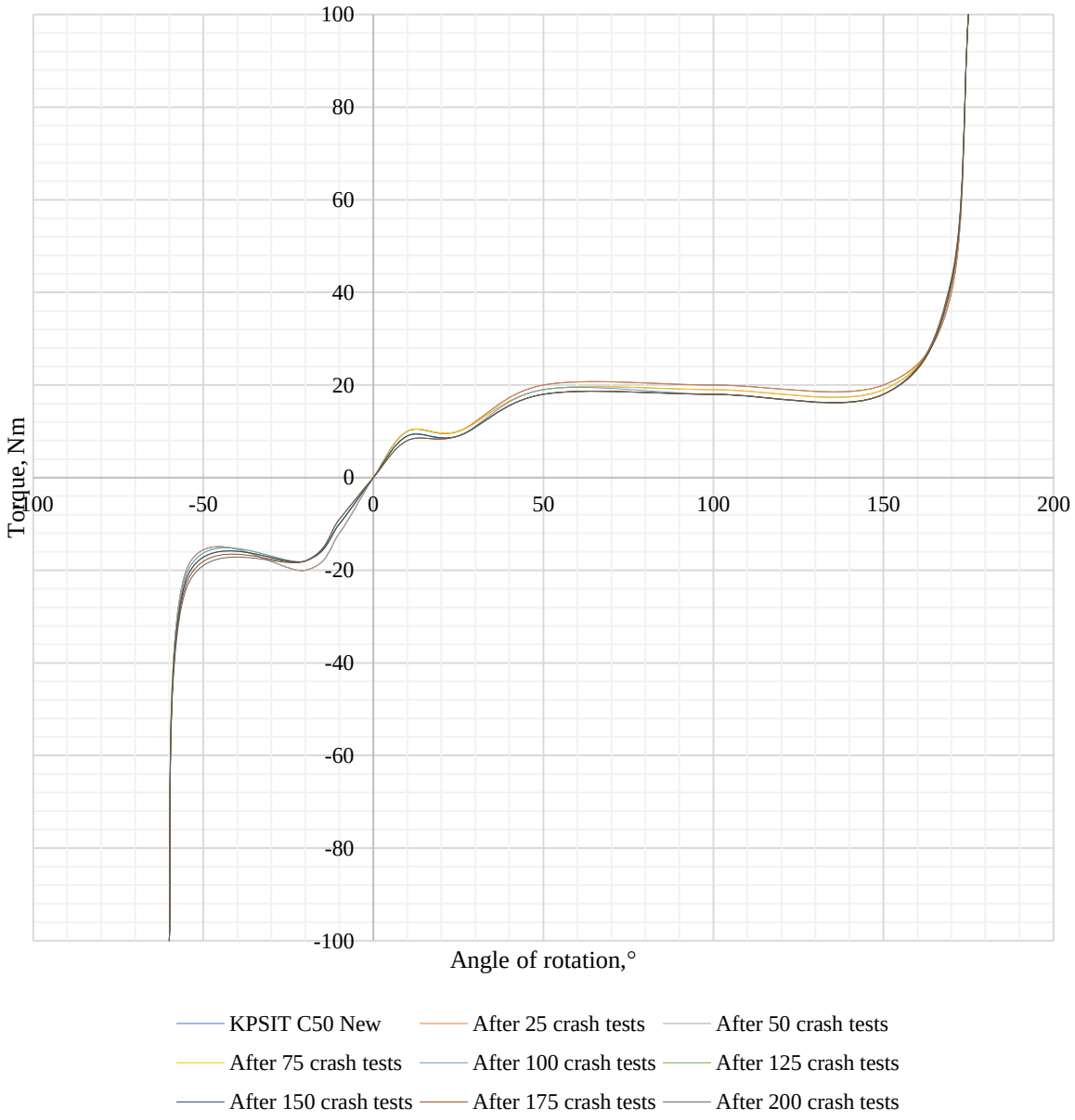

Fig. 24. Characteristics of the drag torque in the shoulder joint of the KPSIT C50 dummy, taking into account a cycles of crash test measurements.

When analyzing the torque of resistance in the shoulder joint of the KPSIT C50 in terms of reliability, it is important to note that after a cycles of 200 crash tests, the KPSIT C50 joint is functional, and its drag torque does not exceed 100Nm. In the case of backward movement of the joint, a reduction in drag torque is only visible after 75 crash tests at a joint rotation angle of 20° and amounts to 18 Nm (Initial value 20 Nm). In the case of backward movement of the joint, an increase in drag torque is only visible after 75 crash tests at a joint rotation angle of 55° and amounts to 21 Nm (initial value of 20 Nm) and after 200 crash tests at a rotation angle of 55° and amounts to 24 Nm (Initial value of 20 Nm). In the case of forward movement of the joint, a reduction in the drag torque is only visible after 50 crash tests at a rotation angle of up to 150° and amounts to 19 Nm (Initial value of 20 Nm). In the case of forward movement of the joint, an increase in drag torque is only visible after 50 crash tests at a joint rotation angle of 170° and is 41 Nm (Initial value 40 Nm) and after 200 crash tests at a rotation angle of 170° and is 43 Nm (Initial value 40 Nm).

The characteristics of the torque of resistance in the knee joint of the KPSIT C50 dummy are shown in Figures 25 to 23. The characteristics of the torque of resistance in the knee joint of the KPSIT C50 dummy, taking into account all cycles of crash test measurements, are shown in Figure 24.

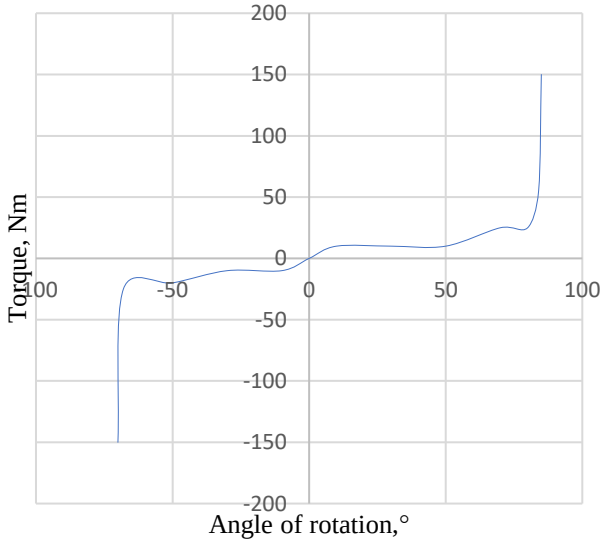

Fig. 25. Characteristics of the torque of resistance in the knee joint of the KPSIT C50 dummy – before the first crash test.

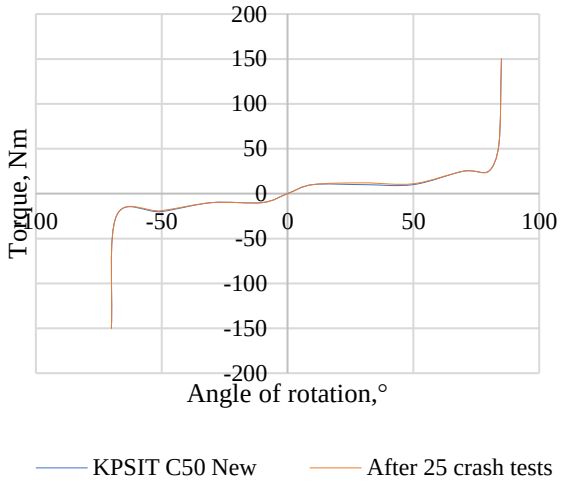

Fig. 26. Characteristics of the drag torque in the KPSIT C50 knee joint – after 25 crash tests.

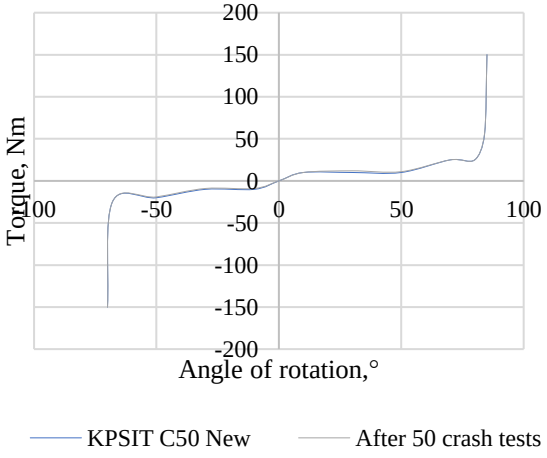

Fig. 27. Characteristics of the drag torque in the KPSIT C50 knee joint – after 50 crash tests.

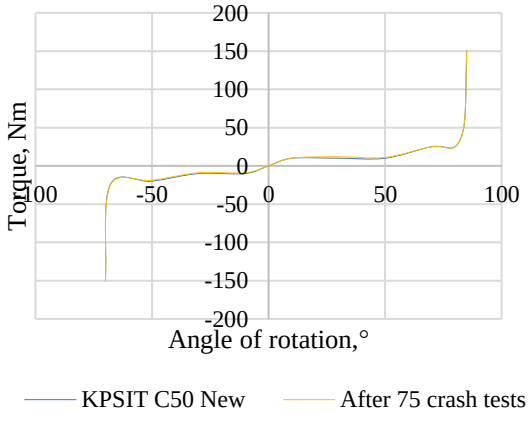

Fig. 28. Characteristics of the drag torque in the KPSIT C50 knee joint – after 75 crash tests.

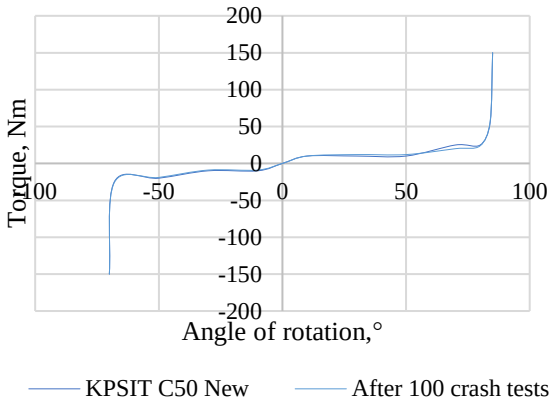

Fig. 29. Characteristics of the drag torque in the KPSIT C50 knee joint – after 100 crash tests.

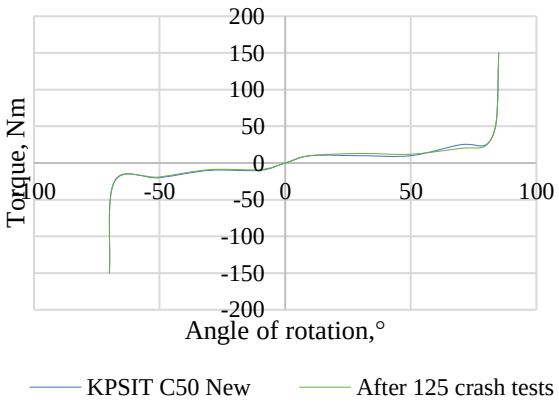

Fig. 30. Characteristics of the drag torque in the KPSIT C50 knee joint – after 125 crash tests.

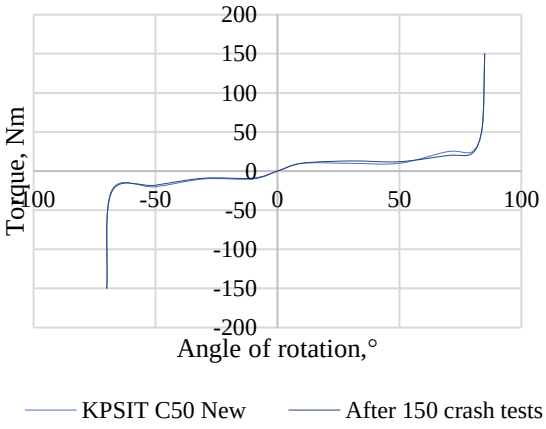

Fig. 31. Characteristics of the drag torque in the KPSIT C50 knee joint – after 150 crash tests.

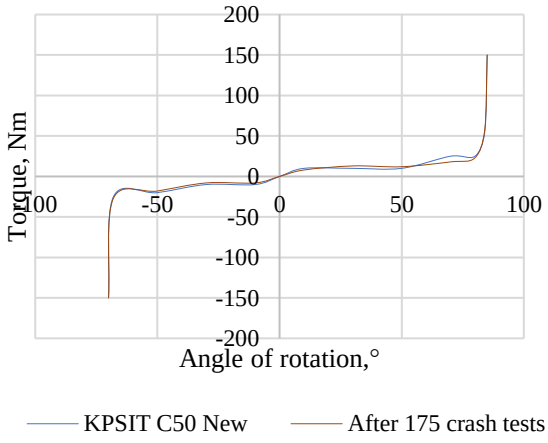

Fig. 32. Characteristics of the drag torque in the KPSIT C50 knee joint – after 175 crash tests.

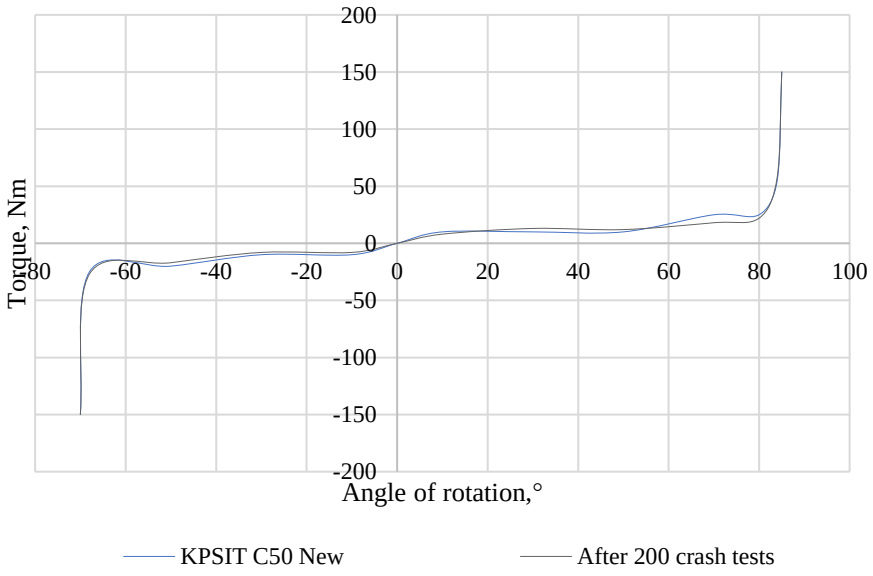

Fig. 33. Characteristics of the drag torque in the KPSIT C50 knee joint – after 200 crash tests.

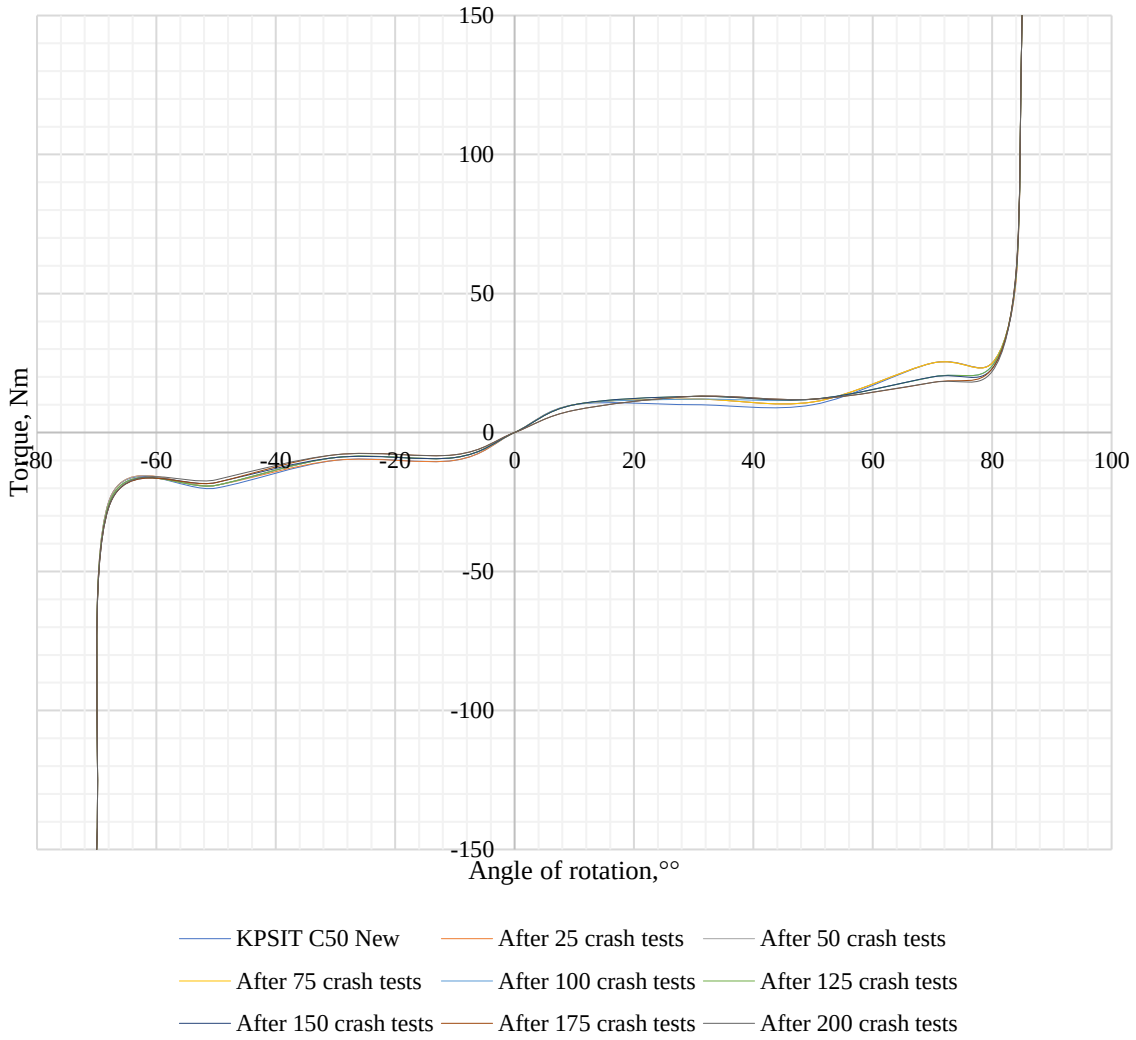

Fig. 34. Characteristics of the drag torque in the knee joint of the KPSIT C50 dummy taking into account a cycles of crash test measurements.

When analyzing the torque of resistance in the knee joint of the KPSIT C50 in terms of reliability, it is important to note that after a cycles of 200 crash tests, the KPSIT C50 joint is in good working order and its drag torque does not exceed 150Nm in the final movements of the joint. In the case of backward movement of the joint, a reduction in the drag torque is only visible after 50 crash tests at a rotation angle of 30° and is 9 Nm (Initial value of 10 Nm). In the case of backward movement of the joint, an increase in drag torque is only visible after 75 crash tests at a joint rotation angle of 68° and is 26 Nm (initial value 25 Nm) and after 200 crash tests at a rotation angle of 68° and is 27 Nm (Initial value 25 Nm). In the case of forward movement of the joint, a reduction in drag torque is only visible after 75 crash tests at a rotation angle of up to 70° and is 20 Nm (Initial value 25 Nm). In the case of forward movement of the joint, an increase in drag torque is only noticeable after 50 crash tests at a pivot angle of 84° and amounts to 56 Nm (initial value of 55 Nm) and after 200 crash tests at a rotation angle of 84° and amounts to 58 Nm (Initial value of 55 Nm).

5. Conclusions

The article presents one of the elements of the comparison of the KPSIT C50 dummy with the Hybrid III 50th centil male dummy and presents changes in the characteristics of the torque of resistance in the joints after a cycles of crash tests.

The paper presents an analysis of the characteristics of the resistance moment in joints during a cycles of crash tests. The results of the analysis show that the vapor characteristics remain virtually unchanged after a cycle of 200 tests.

It has been shown that the use of an innovative solution allows for fast, efficient and trouble-free performance of crash tests at low crash speeds.

The main objective of the study has been confirmed, it has been shown that the joints used in the shoulder and knee joints of the KPSIT C50 dummy remain functional after a cycles of 200 crash tests and do not require calibration of the joint or its replacement with a new one. In addition, it should be noted that the constructed knuckle joint KPSIT C50 can be used in other KPSIT dummy representing the remaining percentile of both male and female populations.

What is also very important: the current Hybrid III dummies are designed for tests at higher crash speeds, starting from 25 km/h in frontal and side crash tests, and at a speed of 16 km/h in the rear test using the BioRid II dummy. Preliminary studies performed on a group of volunteers showed a very good agreement in displacement of the KPSIT C50 dummy with studies on volunteers.

Further research will expand the studies on a larger sample and extend the work to include comparative studies of the KPSIT cervical joint with volunteers and the Hybrid III 50th centil male dummy during crash tests carried out at low speeds.

Reference

1. Van Ratingen, M., Williams, A., Anders, L., Seeck, A., Castaing, P., Kolke, R., Miller, A., The european new car assessment programme: A historical review. *Chinese journal of traumatology*, 2016, 19(02), 63-69. https://doi.org/10.1016/j.cjtee.2015.11.016
2. Parenteau, C. S., Viano, D. C., Burnett, R.. Second-row occupant responses with and without intrusion in rear sled and crash tests. *Traffic injury prevention*, 2021, *22*(1), 43-50. https://doi.org/10.1080/15389588.2020.1842380
3. Kostek, R. Algorithms of identification of car body contact parameters from a movie of crash test. In *AIP Conference Proceedings*, 2023, 2949, 1. https://doi.org/10.1063/5.0165471
4. Murawski J, Szczepański E, Jacyna-Gołda I, Izdebski M, Jankowska-Karpa D. Intelligent mobility: A model for assessing the safety of children traveling to school on a school bus with the use of intelligent bus stops. *Eksploatacja i Niezawodność – Maintenance and Reliability*. 2022;24(4):695-706. https://doi.org/10.17531/ein.2022.4.10
5. Lawton, G. Crash test dummies. *New scientist*, 2018, *238*(3177), 42-43. https://doi.org/10.1016/S0262-4079(18)30846-7
6. Schäuble, Andreas. *Crash test dummies–how realistic are currently used dummies?*. Diss. Wien, 2019.
7. Linder, A., Svensson, M. Y. Road safety: the average male as a norm in vehicle occupant crash safety assessment. *Interdisciplinary Science Reviews*, 2019, *44*(2), 140-153. https://doi.org/10.1080/03080188.2019.1603870
8. Wang, Z. J., Loeber, B., Tesny, A., Hu, G., Kang, Y. S. Neck biofidelity comparison of THOR-AV, THOR and Hybrid III 50th dummies. In *IRCOBI Conference Proceedings* 2021, 8-10.
9. Carroll, J., Kruse, D., Mishra, E., Mroz, K., Lubbe, N. Comparison of Hybrid III and THOR 5th percentile female dummies in frontal crash tests. In *Proceedings of IRCOBI Conference. 2021*.
10. Eggers, A., Schießler, M., Ott, J., Langner, T., Wisch, M. Sensitivity of Chest Deflection Measurements in Thor-5F and Hybrid III Small Female Dummies to Different Seat and Belt Settings. In *27th International Technical Conference on the Enhanced Safety of Vehicles (ESV) National Highway Traffic Safety Administration* 2023, 23-0301.
11. Guan, S., Liao, Z., Xiang, H., Zhu, X., Wang, Z., Zhao, H., Lai, X., Experimental Study of Thoracoabdominal Injuries Suffered from Caudocephalad Impacts Using Pigs. *Applied bionics and biomechanics*, 2018. https://doi.org/10.1155/2018/2321053
12. Gabauer, D., Thomson, R., Correlation of vehicle and roadside crash test injury criteria. In *19th International Technical Conference on the Enhanced Safety of Vehicles (ESV)-Washington DC June* 2005, 6-9.
13. Linder, A., Svensson, M. Y., BioRID, a crash test dummy for rear impact: a review of development, validation and evaluation. In *Proceedings of the 2000 Road Safety Research, Policing and Education Conference, Brisbane, Queensland*., 2000.
14. Lizbetin, J., Stopka, O. Proposal of a Roundabout Solution within a Particular Traffic Operation. Open Engineering, 2016, 6, 1, 441-445, DOI: 10.1515/eng-2016-0066.
15. Malin, F., Norros, I., Innamaa, S., Accident risk of road and weather conditions on different road types. *Accident Analysis & Prevention*, 2019, 122, 181-188. https://doi.org/10.1016/j.aap.2018.10.014
16. Goniewicz, K., Goniewicz, M., Pawłowski, W., Fiedor, P., Road accident rates: strategies and programmes for improving road traffic safety. *European journal of trauma and emergency surgery*, 2016, 42, 433-438. https://doi.org/10.1007/s00068-015-0544-6
17. *The World's First Car Accident*, (in): https://historyofyesterday.com/the-worlds-first-car-accident/?utm_content=cmp-true, access from

23.09.2023

18. Guizzo, Erico. Anatomy of a Crash-Test Dummy, *IEEE Spectrum*, October 2007. https://doi.org/10.1109/MSPEC.2007.4337665
19. Roach, Mary. Stiff: The Curious lives of Human Cadavers. New York: W.W. Norton, 2003
20. *The father of anthropomorphic dummy testing, (in): https://www.humaneticsgroup.com/about-us/history*, access from 23.09.2023
21. Frej D. Analysis of Head Displacement during a Frontal Collision at a Speed of 20 km/h—Experimental Studies. *Sustainability*. 2023; 15(22), 16015. https://doi.org/10.3390/su152216015
22. Jackson, K. E., Boitnott, R. L., Fasanella, E. L., Jones, L. E., Lyle, K. H., A history of full-scale aircraft and rotorcraft crash testing and simulation at NASA Langley Research Center. *In 4th Triennial International Aircraft and Cabin Safety Research Conference*, 2004.
23. Croft, A. C., Philippens, M. M., The RID2 biofidelic rear impact dummy: A pilot study using human subjects in low speed rear impact full scale crash tests. *Accident Analysis & Prevention*, 2007, 39(2), 340-346. https://doi.org/10.1016/j.aap.2006.09.003
24. Woitsch, G., Sinz, W., Influences of pre-crash braking induced dummy – Forward displacements on dummy behaviour during EuroNCAP frontal crashtest. *Accident Analysis & Prevention*, 2014, 62, 268-275. DOI: 10.1016/j.aap.2013.10.012..
25. Gabler, L. F., Crandall, J. R., Panzer, M. B., Assessment of kinematic brain injury metrics for predicting strain responses in diverse automotive impact conditions. *Annals of biomedical engineering*, 2016, 44, 3705-3718. https://doi.org/10.1007/s10439-016-1697-0
26. Sanchez, E. J., Gabler, L. F., McGhee, J. S., Olszko, A. V., Chancey, V. C., Crandall, J. R., Panzer, M. B. Evaluation of head and brain injury risk functions using sub-injurious human volunteer data. *Journal of neurotrauma*, 2017, 34(16), 2410-2424. https://doi.org/10.1089/neu.2016.4681
27. Frej, D., Jaśkiewicz, M., Comparison of Volunteers' Head Displacement with Computer Simulation—Crash Test with Low Speed of 20 km/h. *Sensors,* 2022, 22(24), 9720. https://doi.org/10.3390/s22249720
28. Podosek K, Frej D, Górniak A, Elvira N. 50 percentile dummy movement analysis using TEMA Automotive software. The Archives of Automotive Engineering – Archiwum Motoryzacji. 2022;97(3):25-50. doi:10.14669/AM/155002.
29. Bruski, D., Burzyński, S., Chróścielewski, J., Jamroz, K., Pachocki, Ł., Witkowski, W., Wilde, K., Experimental and numerical analysis of the modified TB32 crash tests of the cable barrier system. *Engineering failure analysis*, 2019, 104, 227-246. https://doi.org/10.1016/j.engfailanal.2019.05.023
30. Górniak, A.; Matla, J.; Górniak, W.; Magdziak-Tokłowicz, M.; Krakowian, K.; Zawiślak, M.; Włostowski, R.; Cebula, J. Influence of a Passenger Position Seating on Recline Seat on a Head Injury during a Frontal Crash. *Sensors* 2022, 22, 2003. https://doi.org/10.3390/s22052003
31. *Przegub barkowy manekina antropometrycznego do testów zderzeniowych,* (Shoulder joint of the anthropometric crash test dummy Application), Zgłoszenie oznaczono numerem: P.433041,[WIPO ST 10/C PL433041].
32. *Przegub kolanowy manekina antropometrycznego do testów zderzeniowych*, (Knee-joint of the anthropometric crash test dummy), Zgłoszenie oznaczono numerem: P.431522,[WIPO ST 10/C PL431522].
33. Prochowski, L., Dębowski, A., Żuchowski, A., Zielonka, K., Evaluation of the influence of velocity on dynamic passenger loads during a frontal minibus impact against an obstacle. *In IOP Conference Series: Materials Science and Engineering, 2016,* 148, 1, 012024). IOP Publishing. https://doi.org/10.1088/1757-899X/148/1/012024
34. Frej DP, Zuska A. The impact of the Covid -19 pandemic on the frequency of vehicle accidents in Poland. *The Archives of Automotive Engineering – Archiwum Motoryzacji.* 2023;99(1):30-44. doi:10.14669/AM/162666.
35. Stopka, O., Stopkova, M., Kampf, R., Application of the Operational Research Method to Determine the Optimum Transport Collection Cycle of Municipal Waste in a Predesignated Urban Area. *Sustainability*, 2019, 11(8), Article no: 2275. DOI: 10.3390/su11082275.
36. Borucka A, Pyza D. Influence of meteorological conditions on road accidents. A model Indexed by: for observations with excess zeros. Eksploatacja i Niezawodność – Maintenance and Reliability. 2021;23(3):586-92. https://doi.org/10.17531/ein.2021.3.20
37. Świderski A., Borucka A., Skoczyński P. Characteristics and Assessment of the Road Safety Level in Poland with Multiple Regression Model, Transport Means part I, 2018, Lithuania 2018, 92 - 97
38. Gorzelanczyk, P., Tylicki, H. Forecasting the Number of Road Accidents in Poland Depending on the Day of the Week using Neural Networks. *LOGI – Scientific Journal on Transport and Logistics*, 2023, 14(1), 35-42. DOI: 10.2478/logi-2023-0004.
39. Szumska EM, Pawełczyk M, Jurecki R. Total Cost of Ownership analysis and energy efficiency of electric, hybrid and conventional urban

buses. *Eksploatacja i Niezawodność – Maintenance and Reliability*. 2022;24(1):7-14. https://doi.org/10.17531/ein.2022.1.2.

40. Joszko, K., Wolański, W., Burkacki, W., Suchoń, S., Zielonka, K., Muszyński, A., Gzik, M., Biomechanical analysis of injuries of rally driver with head supporting device. *Acta of bioengineering and biomechanics*, 2016, 18(4), 159-169.
41. Kozłowski E, Borucka A, Oleszczuk P, Jałowiec T. Evaluation of the maintenance system readiness using the semi-Markov model taking into account hidden factors. Eksploatacja i Niezawodność – Maintenance and Reliability. 2023;25(4). https://doi.org/10.17531/ein/172857
42. Borucka A. Three-state Markov model of using transport means, Business Logistics in Modern Management, 2018, 18, 3-19, ISSN 1849-5931
43. Karwala Ł. Analysis of the selection of a child seat. *The Archives of Automotive Engineering – Archiwum Motoryzacji*. 2023;101(3):86-95. https://doi.org/10.14669/AM/172370